

OAK RIDGE NATIONAL LABORATORY LIBRARIES



3 4456 0555879 5

ORNL TM-5337

Cy1

Radiation Insult to the Active Bone Marrow as Predicted by a Method of CHORDS

T. D. Jones

OAK RIDGE NATIONAL LABORATORY
CENTRAL RESEARCH LIBRARY
DOCUMENT COLLECTION
LIBRARY LOAN COPY
DO NOT TRANSFER TO ANOTHER PERSON
If you wish someone else to see this
document, send in name with document
and the library will arrange a loan.
UCR-7889
12-2-67

OAK RIDGE NATIONAL LABORATORY
OPERATED BY UNION CARBIDE CORPORATION FOR THE ENERGY RESEARCH AND DEVELOPMENT ADMINISTRATION

Printed in the United States of America: Available from
National Technical Information Service
U.S. Department of Commerce
5285 Port Royal Road, Springfield, Virginia 22161
Price: Printed Copy \$4.00; Microfiche \$2.25

This report was prepared as an account of work sponsored by the United States Government. Neither the United States nor the *Energy Research and Development Administration*, nor any of their employees, nor any of their contractors, subcontractors, or their employees, makes any warranty, express or implied, or assumes any legal liability or responsibility for the accuracy, completeness or usefulness of any information, apparatus, product or process disclosed, or represents that its use would not infringe privately owned rights.

ORNL/TM-5337

Contract No. W-7405-eng-26

HEALTH PHYSICS DIVISION

RADIATION INSULT TO THE ACTIVE BONE MARROW
AS PREDICTED BY A METHOD OF CHORDS

T. D. Jones

MARCH 1976

NOTICE This document contains information of a preliminary nature and was prepared primarily for internal use at the Oak Ridge National Laboratory. It is subject to revision or correction and therefore does not represent a final report.

OAK RIDGE NATIONAL LABORATORY
Oak Ridge, Tennessee 37830
operated by
UNION CARBIDE CORPORATION
for the
ENERGY RESEARCH AND DEVELOPMENT ADMINISTRATION

OAK RIDGE NATIONAL LABORATORY LIBRARIES



3 4456 0555879 5

TABLE OF CONTENTS

	<u>Page</u>
List of Tables.	iv
List of Figures	iv
Abstract.	1
Introduction to the CHORD Concept	1
CHORD Applications to Red Bone Marrow	3
CHORD Distribution and Marrow Doses	7
Other CHORD Applications.	21
Conclusions	23
Acknowledgments	24
References.	25

LIST OF FIGURES

<u>Figure</u>	<u>Page</u>
1. <u>Critical Human Organ Radiation Dosimetry</u> the CHORD Concept.	4
2. Distributions of the Active Bone Marrow.	5
3. CHORD Density Functions for Active Marrow in Reference Man . . .	8
4. Dose to Active Marrow as Predicted by the CHORD Concept. . . .	11
5. Active Marrow Dose Relative to Exposure at the Front of the Chest (A-P Exposure)	12
6. Photon Attenuation of Skeletal Tissue Compared to that of Soft Tissue.	14
7. Dose to Bone Marrow from a Broad Beam Incident on a Rotating Phantom	16
8. Dose from Recoil Ions to the Active Marrow as Predicted by the CHORD Concept	20
9. Critical Human Organ Radiation Dosimeter	22

LIST OF TABLES

<u>Table</u>	<u>Page</u>
1. CHORD $p\{\ell\}\Delta\ell$ Values for Active Marrow in Reference Man	9
2. Active Marrow Dose Relative to Dose at the Front of the Chest.	15
3. Dose to Active Marrow from Neutron Produced Recoil Ions as Predicted by CHORD Distributions.	19

CRITICAL HUMAN ORGAN RADIATION DOSIMETRY FOR THE
ACTIVE BONE MARROW*

Abstract

Critical Human Organ Radiation Dosimetry (CHORD) probability density functions for A-P, P-A, bilateral, rotational, and isotropic incidence, plus simple depth-dose data, permit the rapid estimation of the radiation insult to the active red bone marrow system of the ICRP Reference Man. The CHORD concept follows the variations in the microscopic processes of absorption, attenuation, and scattering on a macroscopic level so that it is not necessary to attempt detailed calculations for each and every case of interest. Similar techniques have been applied to reactor criticality calculations and the general logic of the CHORD process can be applied to any cause-response type situation which can be described in terms of variation with distance in the medium of interest. Doses to active bone marrow from exposures to photons and neutrons are presented and excellent agreement was found with the few available experimental results.

Introduction to the CHORD Concept

When a bioorganism is subjected to a radiation environment, a critical organ or region of greatest risk usually is irradiated non-uniformly if the linear dimensions of the critical organ are not small or the depth of the critical organ within the bioorganism is not large compared with the mean-free pathlengths of the irradiating particles. Radiation insult specific analyses are usually based on dose to cells,

*Research sponsored by the Energy Research and Development Administration under contract with Union Carbide Corporation.

a small target site or cluster of cells within an organ such as the mandible, or a center such as the central nervous, or active bone marrow system. For some effects, cells or sensitive sites within cells may not be irradiated uniformly because of discrete energy loss events and microdosimetric considerations (Rossi, 1975) may be desirable. On a more macroscopic scale, chronic effects such as bone sarcomas or even leukemia may, in some cases, be directly related to highly localized exposures such as usually encountered in radiotherapy of tumors and the maximum absorbed dose at a particular site (mass of a gram as opposed to an intercellular site) may be more meaningful than the mean absorbed dose to the complete active marrow system (Wilson and Carruthers, 1962; A. R. Jones, 1975). Detailed distribution of photon dose to specific active marrow regions for A-P, P-A, rotational, and side (lateral) incidence have been published and should be readily applied to many situations of interest (Jones et al., 1973; Clifford and Facey, 1970). For radiation protection and risk analyses from acute effects and those chronic effects where risk is thought to be proportional to the insult to the system such as usually assumed for leukemia, it is often not possible or desirable to establish insult-response type correlations on a microscopic level. Therefore, it becomes necessary to assign a "mean" insult or risk to a non-uniformly irradiated "critical organ".

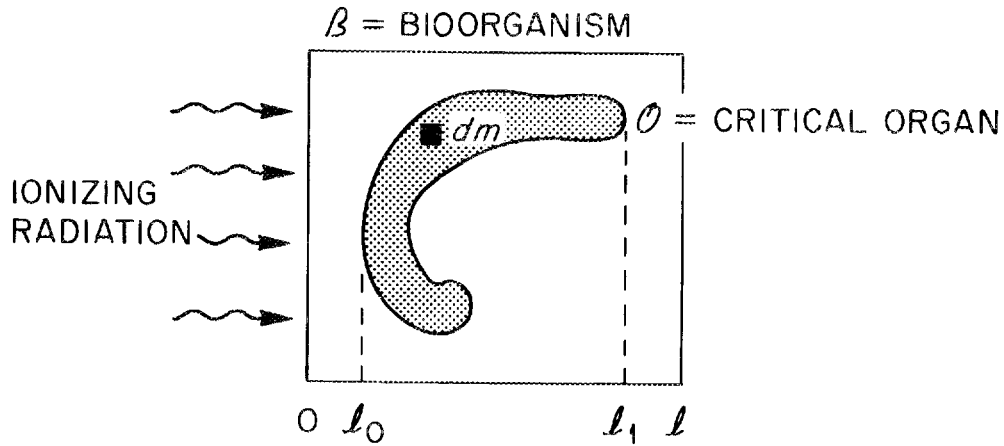
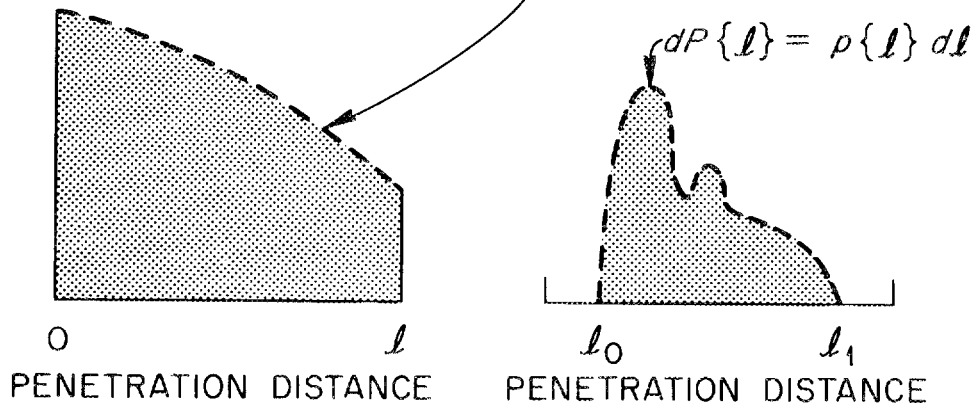
One approach to the dosimetry of a non-uniformly irradiated critical organ, such as the red bone marrow system, is to use a probability density distribution of length, referred to as a CHORD length distribution. Any specific CHORD or $p\{l\}$ dl distribution is

obtained by assuming that the critical organ is simply a volume of constant density, and for each differential unit of mass dm , chosen by Monte Carlo techniques, the minimum distance ℓ to the closest irradiated air-tissue interface is uniquely determined. This process is continued until $p\{\ell\} d\ell$ is well known statistically. Chord usually implies a straight line through two points on the surface, e.g., the skin; however, in this paper CHORD is an acronym derived from Critical Human Organ Radiation Dosimetry and represents only a specific portion of a "true Chord". The CHORD concept is illustrated in Figure 1 and the CHORD or $p\{\ell\} d\ell$ distribution provides "weighting" factors for an integration over a specific insult such as a "multicollision" depth-dose curve for the source geometry of interest.

CHORD Applications to Red Bone Marrow

Figure 2 illustrates the distribution of the active red bone marrow in the normal adult and the corresponding analog for our Monte Carlo transport code. In the adult reference man (ICRP, 1975) there are 1500 grams of active red marrow and 1500 grams of yellow marrow which are predominately fat cells. Inactive yellow marrow may be transformed quickly into active marrow by a stimulus such as bleeding or infection; yellow marrow in bone shafts is known to contain some active cells but, in general, the proportion of active cells in adult yellow marrow is usually considered to be small (Spiers, 1966). Thus, for most situations of interest, only the red marrow receives major consideration.

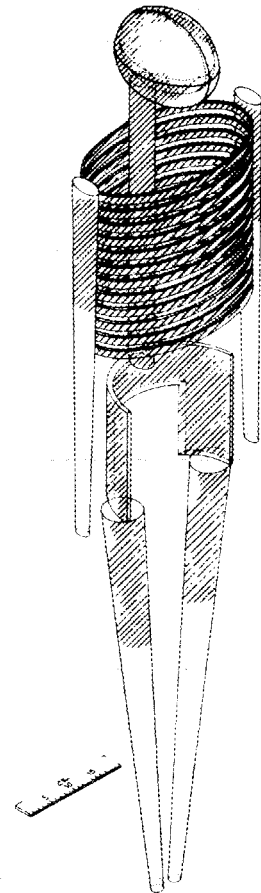
ORNL - DWG 75-7339

MULTICOLLISION DOSE = $D(l)$ BUT $l = l(dm)$,

$$\text{AND } \bar{D} = \int_0^{\infty} D(l) \cdot p\{l\} \cdot dl / \int_{-\infty}^{\infty} p\{l\} \cdot dl$$

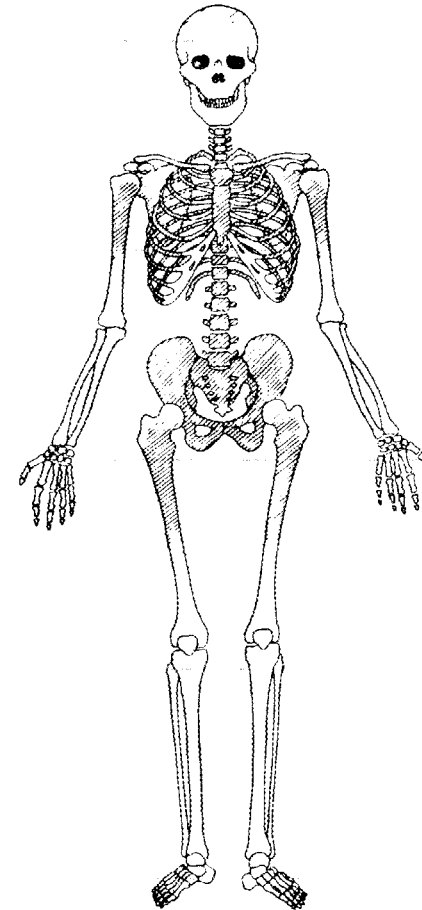
Fig. 1. Critical Human Organ Radiation Dosimetry the CHORD Concept.

ORNL-DWG 70-4810



COMPUTER ANALOG OF
REFERENCE MAN

SKULL	13.1%
VERTEBRAE	28.4%
RIBS + STERNUM	10.2%
SCAPULAE	4.8%
HEAD AND NECK OF BOTH ARMS	1.9%
BOTH CLAVICLES	1.6%
HEAD AND NECK OF BOTH LEGS	3.8%
PELVIS	36.2%
TOTAL AMOUNT OF RED BONE MARROW: 1500 g	
 RED BONE MARROW	



A NORMAL ADULT
(HASHIMOTO 1060)

Fig. 2. Distributions of the Active Bone Marrow.

The importance of a risk estimate based on radiation damage to the active marrow system cannot be overstated as bone marrow damage usually will be the major mechanism in radiation death and acute radiation sickness stemming from whole body irradiation because it occurs at much lower levels (Facey, 1968; Wald, 1975) than death or incapacitation due to radiation damage of the gut mucosa or the central nervous system. For sublethal criticality accident exposure levels, levels of interest in radiation protection, and population exposure levels, the most demanding recommendations of the ICRP (1964) relate to the maximum permissible doses to the gonads and the blood-forming organs. In radiation protection, the testes are usually considered to be the critical organ of primary interest because of their shallow location and because of the difficulty of estimating the bone marrow insult; however, if the exposure level subjects an individual to considerable risk, then an estimation of the insult to his active marrow system could be advantageous for determining what medical treatment should be administered promptly (Wald, 1975).

The dose at a penetration depth of 5 cm is often chosen to describe the insult to the red bone marrow; however, for photon irradiation the "5 cm rule" is often in error by a factor of two and is expected to be even worse for neutron irradiation. This approximation tends to retain popularity in spite of its inaccuracy, because the red marrow is distributed widely in the skeleton. The skeletal distribution shown in Figure 2 illustrates the fact that, in general, no specific depth can be applied for different exposure

geometries and different irradiating particles or even different energies of particles having the same nature.

For internal dosimetry, especially for radionuclides deposited in or near the skeleton, a precise calculational analog of the active marrow system requires some postulations about cavity size variation and the distribution of these marrow cavities within the skeleton. However, for most situations of external exposure, the active marrow may be assumed to be uniformly deposited in certain regions of the skeleton. This simplification is possible because for external exposure, distance versus insult (dose) variation is much less than for internal radionuclide deposition where the insult (dose) usually varies even more rapidly than inversely with the square of the distance. There are two opposing effects that also influence the photon absorbed dose to marrow. These effects are the increased shielding by the bone structure and the enhancement of dose near the higher atomic number bone tissue (Spiers, 1966; Wilson and Carruthers, 1962). As demonstrated later, the net influence of these opposing effects is usually considered to be small for external exposure although such is not always the case for internal emitters.

CHORD Distribution and Marrow Doses

Figure 3 and Table 1 present CHORD density functions for active marrow in the Reference Man Phantom (ICRP, 1975) for A-P, P-A, bilateral, rotational, and isotropic exposure. Due to the nature of the CHORD concept and the general convexness of the Reference Man Phantom, there is no differentiation between 2π and 4π CHORD distributions; however, depth-dose curves will reflect the different

ORNL-DWG 75-7924R

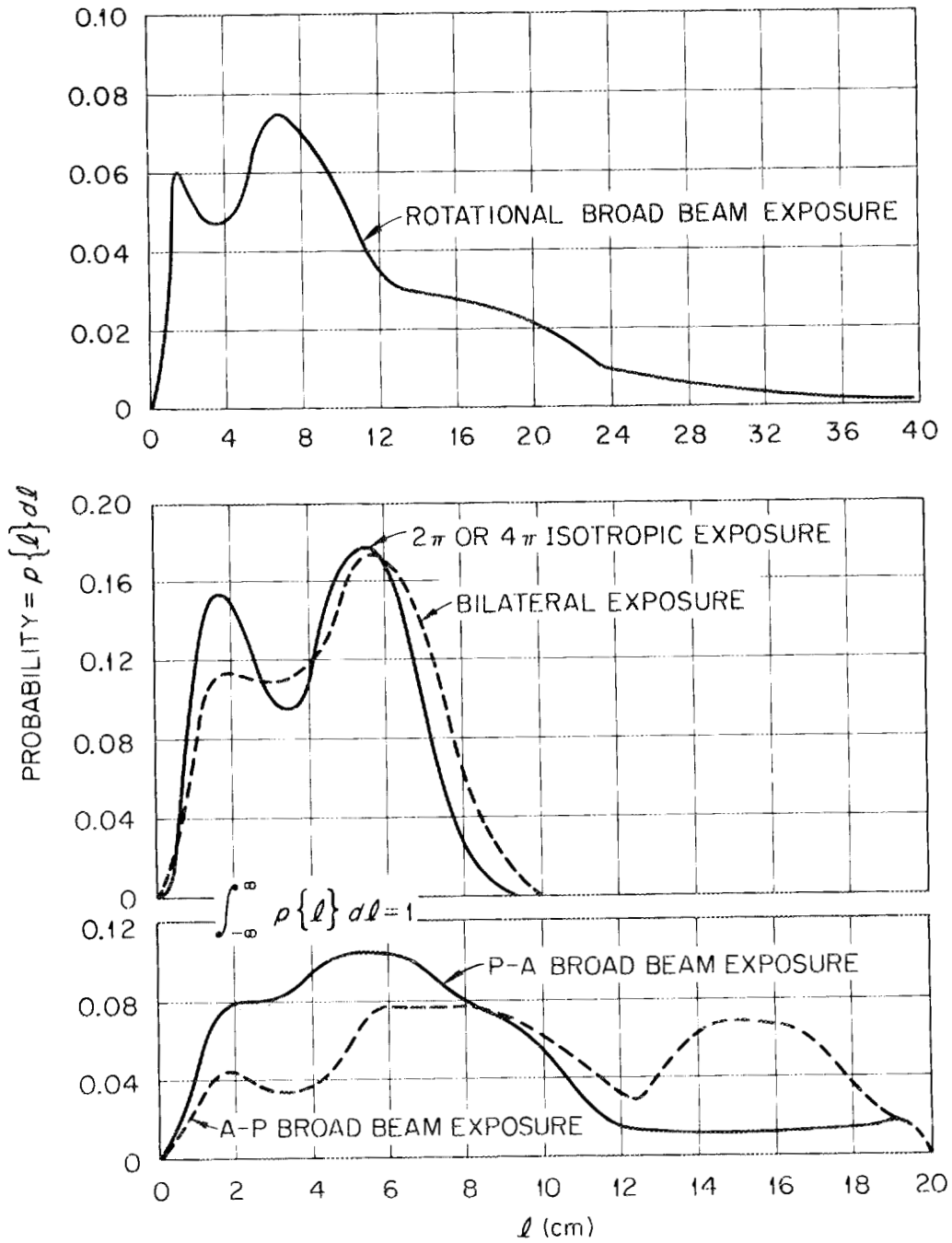


Fig. 3. CHORD Density Functions for Active Marrow in Reference Man.

Table 1. CHORD $p\{\ell\}\Delta\ell$ Values for Active Marrow in Reference Man.

ℓ (cm)	Rotational	cv	A-P	cv*	P-A	cv	Bilateral	cv	Isotropic	cv
0-0.5	.00515	6	.00626	3	.00718	3	0.0138	2	.0231	3
0.5-1	.0175	3	.0157	2	.0252	1	.0420	1	.0658	2
1-2	.0608	2	.0412	2	.0716	1	.115	1	.154	2
2-3	.0508	3	.0361	2	.0791	1	.114	1	.126	2
3-4	.0465	3	.0340	2	.0850	1	.110	1	.0944	2
4-5	.0505	3	.0442	2	.107	1	.133	1	.152	2
5-6	.0662	2	.0730	1	.126	1	.173	1	.179	2
6-7	.0744	2	.0782	1	.109	1	.160	1	.136	2
7-8	.0705	2	.0748	1	.0806	1	.0966	1	.0586	2
8-9	.0703	2	.0738	1	.0756	1	.0359	2	.0105	6
9-10	.0603	2	.0641	1	.0626	1	.00688	4		
10-11	.0482	3	.0522	1	.0440	2				
11-12	.0380	3	.0364	2	.0207	2				
12-13	.0311	3	.0292	2	.0127	3				
13-14	.0292	3	.0549	1	.0121	3				
14-15	.0282	3	.0658	1	.0119	3				
15-16	.0268	4	.0675	1	.0123	3				
16-17	.0285	3	.0643	1	.0129	3				
17-18	.0283	3	.0492	1	.0130	3				
18-19	.0237	4	.0231	2	.0154	3				
19-20	.0241	4	.0159	3	.0168	2				
20-21	.0218	4								
21-22	.0169	4								
22-23	.0135	5								
23-24	.00985	6								
24-25	.00866	6								
25-26	.00787	7								
26-27	.00672	7								
27-28	.00699	7								
28-29	.00545	8								
29-30	.00562	8								
30-31	.00385	9								
31-32	.00276	11								
32-33	.00194	13								
33-34	.00170	14								
34-35	.00147	15								
35-36	.00184	14								
36-37	.00126	16								
37-38	.00164	14								
38-39	.000988	19								
39-40	.000341	32								

*Coefficient of variation in percent.

exposure geometries. The peak at 2 cm for rotational and isotropic exposure is due to the shorter penetration distances to the side ribs and upper arm bones while the more important peak at about 6 cm is predominantly from the vertebrae and pelvis. The CHORD distributions are influenced strongly by the pelvic region and the thoracic vertebrae which contain about 36% and 28%, respectively, of the total active marrow. In Figure 3, ℓ varies to 40 cm for rotational exposure because it was assumed that rotational CHORD dose estimates will be obtained from broad beam depth-dose data. For bilateral and isotropic exposures, ℓ varies to 10 cm because depth-dose data is expected to be related to the minimum distance to the closest irradiated surface.

The CHORD distributions from Figure 3 were used in conjunction with depth-dose curves (see Figure 1) according to

$$D_{\text{red marrow}} = \sum_{\ell} D(\ell) \cdot p\{\ell\} \cdot \Delta\ell$$

because all CHORD distributions were normalized to unity. Photon dose to the active marrow as predicted by the CHORD concept is shown in Figure 4; however, bilateral and rotational results are not shown because of close agreement with the results for A-P exposure.

Figure 5 provides active marrow dose relative to exposure at the front of the chest for A-P incidence. Alun Jones' experimental results (1964) are included and the mean deviation between the two methods is only 6% to 1.25 MeV which is high into the Compton range

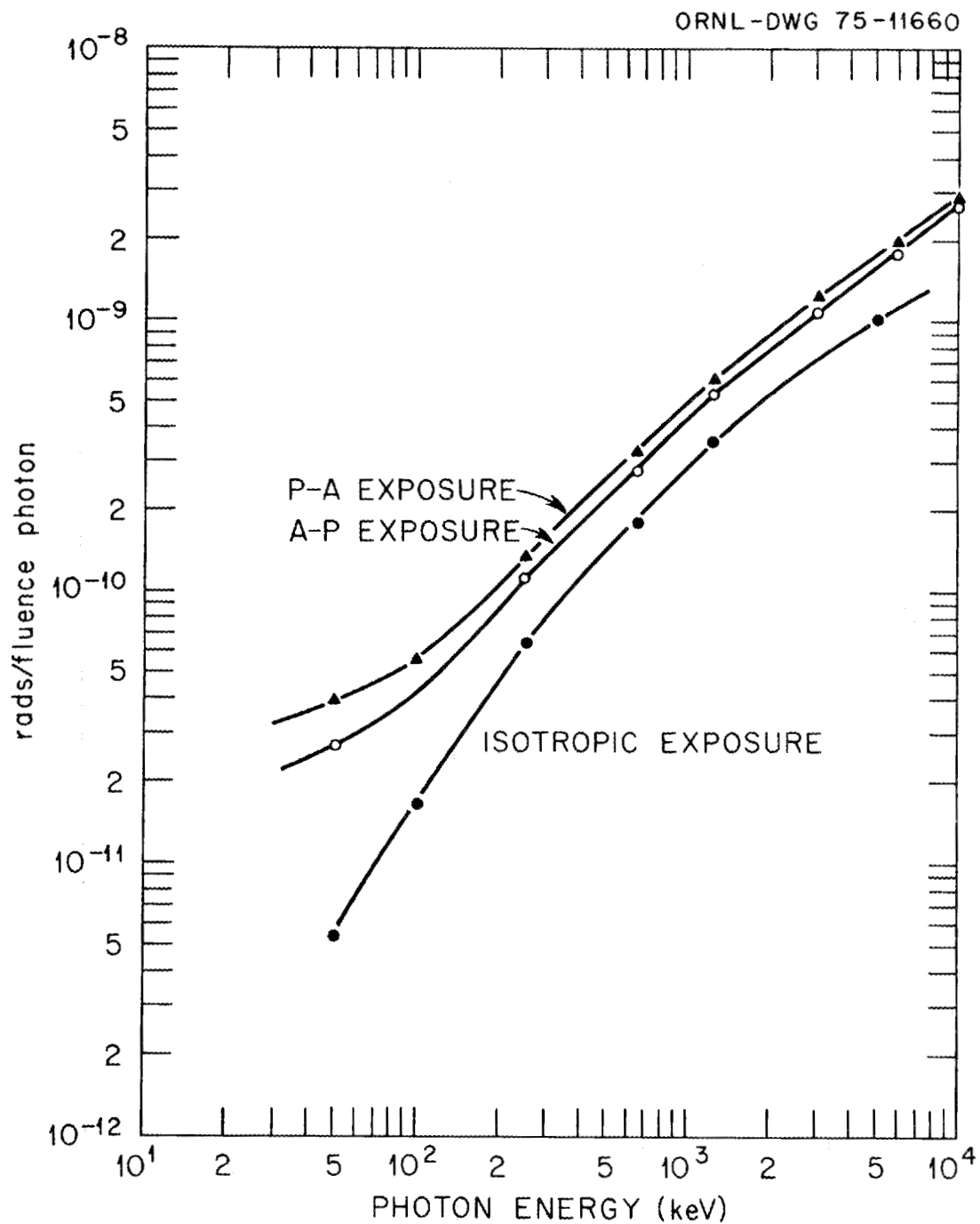


Fig. 4. Dose to Active Marrow as Predicted by the CHORD Concept.

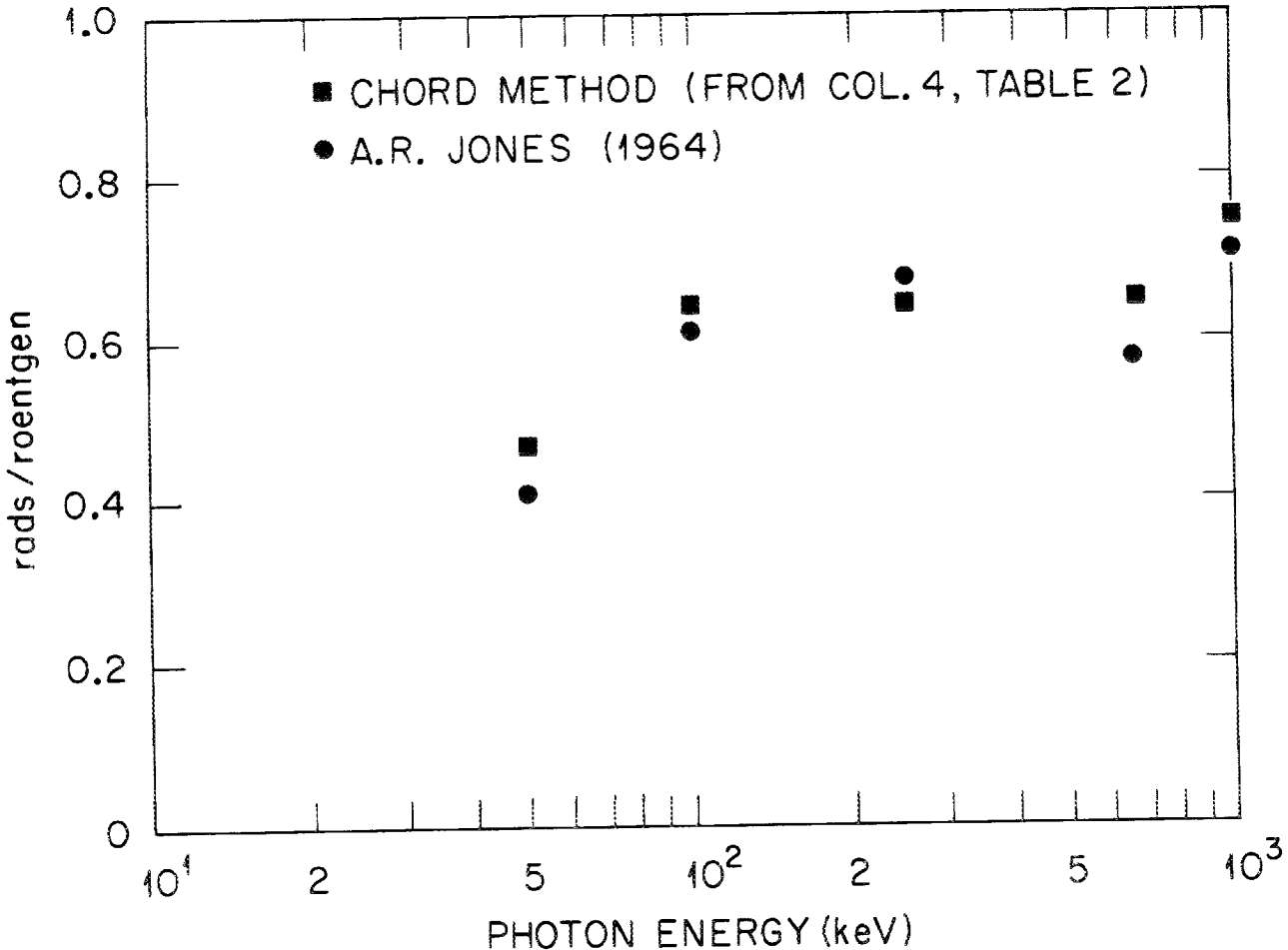


Fig. 5. Active Marrow Dose Relative to Exposure at the Front of the Chest (A-P Exposure).

shown in Figure 6. Figure 6 is intended to serve as a guideline for applications of the method of CHORDs to critical regions in or near bone tissue. Experimental results were not available for higher energies. Column 4 in Table 2 represents estimates from the CHORD method and column 5 is from our Monte Carlo transport code (Jones, et al., 1973). These values shown in column 5 were calculated at the time of the cited reference but have not been published previously in this form. The Monte Carlo results show excellent agreement in the photoelectric region (see Figure 6) but seem to become increasingly inaccurate in the Compton region. This unexpected characteristic of the Monte Carlo results defies explanation at this time but the effect will be investigated.

The important practical case of dose to the active marrow from broad beam incidence on a constantly rotating phantom is shown in Figure 7. Experimental results from Wilson and Carruthers (1962), Alun Jones (1964), and Facey (1968) may have suffered slight disfigurations due to replotting, but all appear to have been normalized to the same ordinate at 250 keV. Much concern has been expressed (Facey 1968) about whether marrow dose per unit exposure should increase monotonically with energy as noted by Wilson and Carruthers (1962) or whether it should peak at about 100 keV as noted by Alun Jones (1964). The different shapes have been considered due to energy degradation within the phantom and the fact that the detector systems of Alun Jones (1964) and Wilson and Carruthers had energy dependences in opposite directions (Facey, 1968).

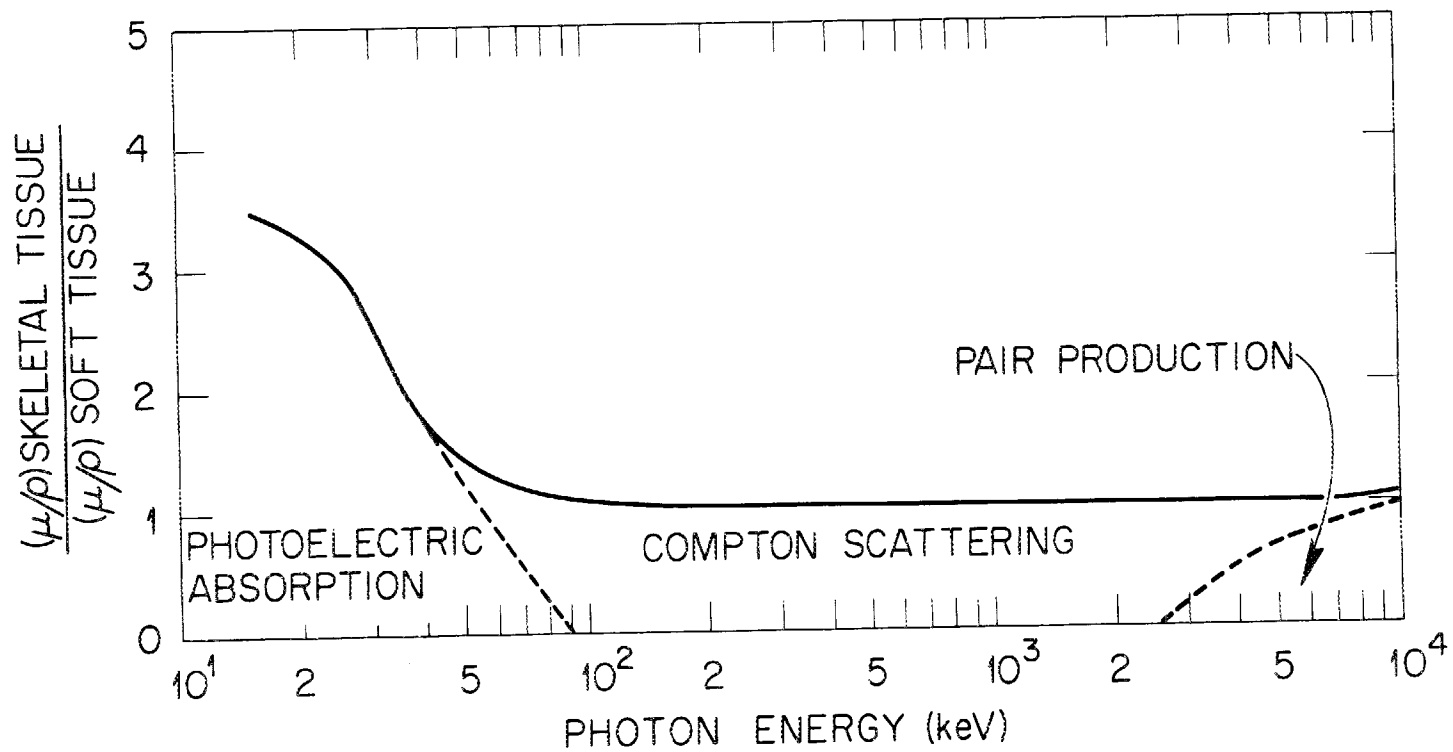


Fig. 6. Photon Attenuation of Skeletal Tissue Compared to that of Soft Tissue.

Table 2. Active Marrow Dose Relative to Dose at the Front of the Chest.

γ -ENERGY	\bar{D} (MARROW)	D^+ (CHEST)	CHORD	\bar{D}/D	MONTE CARLO ⁺⁺
50 KEV	.26*	.48	.54		.54
100	.42	.57	.74		.68
250	1.1	1.47	.75		.47
660	2.7	3.61	.75		.50
1.25 MEV	5.3	6.14	.86		.55

* 10^{-10} RADS/FLUENCE PHOTON

⁺T. D. JONES, HEALTH PHYSICS, 1973, VOL. 24, P. 248.

⁺⁺CALCULATED AT TIME OF HEALTH PHYSICS, VOL. 24, P. 248, 1973, BUT UNPUBLISHED.

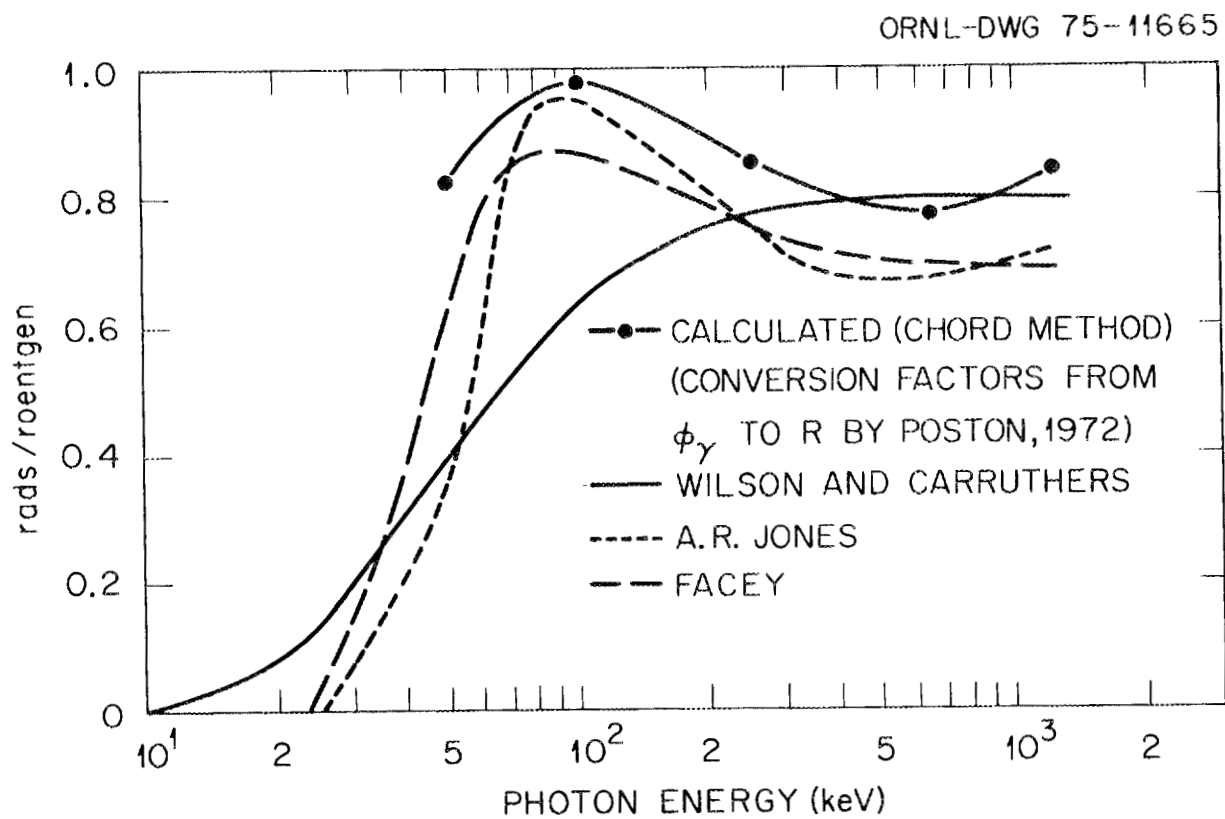


Fig. 7. Dose to Bone Marrow from a Broad Beam Incident on a Rotating Phantom.

At this time, it seems more probable that the different shapes are due primarily to the fact that if one considers the shape of the curve describing the ratio of the photon fluence per unit exposure as a function of photon energy (Rad. Health Hbk, 1970; Fair, 1967) then the dose response curve must have a shape that peaks about 100 keV because the fluence per unit exposure varies more rapidly with energy than does the absorbed dose to the marrow, and secondarily to the fact that Wilson and Carruthers assumed that 60% of the active marrow received a dose similar to that measured in the thoracic vertebrae and 40% received a dose similar to that measured in the sternum*. The CHORD doses are in excellent agreement with Facey's results (1968), except for a consistent 12% overestimation. This deviation is attributed to the facts that (a) 13.1% of the active marrow is in the skull (see Figure 2) which Facey did not include, (b) experimental results from Facey appear to have been normalized to other experimental results at 250 keV, (c) experimentally obtained doses to the active marrow system necessitate the assumption of an "effective mass center" of each important marrow region (Clifford and Facey, 1970)** , and (d) the CHORD estimate did not allow for increased attenuation by bone tissue shielding the marrow. As seen in Figure 6,

*This method of averaging would tend to underestimate dose at lower energies because as Facey (1968) points out, the "pelvis dominates dose at higher energies followed by the thoracic vertebrae and sacrum down to 30 keV. There the ribs enter second place and below 30 keV the ribs dominate." Facey (1968) attempted to resolve difficulties in the rotational case and his results are shown in Figure 7.

**For precision, this "effective mass center" would have to be "weighed" proportionally to dose variations in the local volume of interest; however, most experimenters appear to have used the mass centroid.

this effect is not large except for extremely low energies. At the low energies, dose to the shallow marrow becomes increasingly important, as is shown by the rapid attenuation of dose as a function of depth, and most experimental results are expected to be somewhat low because of the method of averaging. CHORD dose values were normalized per unit exposure according to the Rad. Health Hdbk. (1970)*. In spite of factors a, b, c, and d, excellent agreement for A-P estimates (A. R. Jones, 1964) and rotational estimates (Facey, 1968) compared with the method of CHORDs is observed. Figure 4, which shows the dose to the active marrow for exposure to monoenergetic photons, suggests that if one is concerned only about protection of his bone marrow, he should not do the instinctive thing and turn his back, but instead should face the hazard while backing away. The same effect was also observed by Piesch (1968) and holds for the neutron data in Table 3 which illustrates dose to the active marrow from exposure to monoenergetic neutrons. Some of the data in Table 3 are plotted in Figure 8 for ease of application. Bilateral and rotational results are not shown in Figure 8 because of their close agreement with the results for A-P exposure. Absorbed dose from neutron produced recoil ions is usually characterized by the hydrogen atomic density, because about 70% of the absorbed dose is due to interactions with hydrogen atoms for neutron energies below 14 MeV (Auxier, 1968; Jones, 1974). Standard soft muscle tissue contains about 10% by

* Poston's conversion values of fluence per unit exposure for the Reference Man tissue composition are, for all practical purposes, equal to those in the Rad. Health Handbook.

Table 3. Dose to Active Marrow from Neutron Produced Recoil Ions
as Predicted by CHORD Distributions.

ENERGY	FREE-SPACE* KERMA	P-A**	A-P	BILATERAL	ROTATIONAL	ISOTROPIC
.025 eV	2.1	2.1	1.2	1.4	1.6	.70
1 KEV	1.0	3.3	2.2	2.1	2.3	1.1
10 KEV	10.	4.1	2.6	2.6	2.8	1.6
100 KEV	70.	12.	7.4	9.4	9.2	5.4
1 MeV	230.	110.	67.	74.	75.	47.
2.5 MeV	340.	240.	180.	150.	190.	84.
14 MeV	690.	590.	520.	420.	540.	330.

* $\times 10^{-9}$ ERGS/(GRAM-FLUENCE NEUTRON)

** $\times 10^{-11}$ RADS/FLUENCE NEUTRON

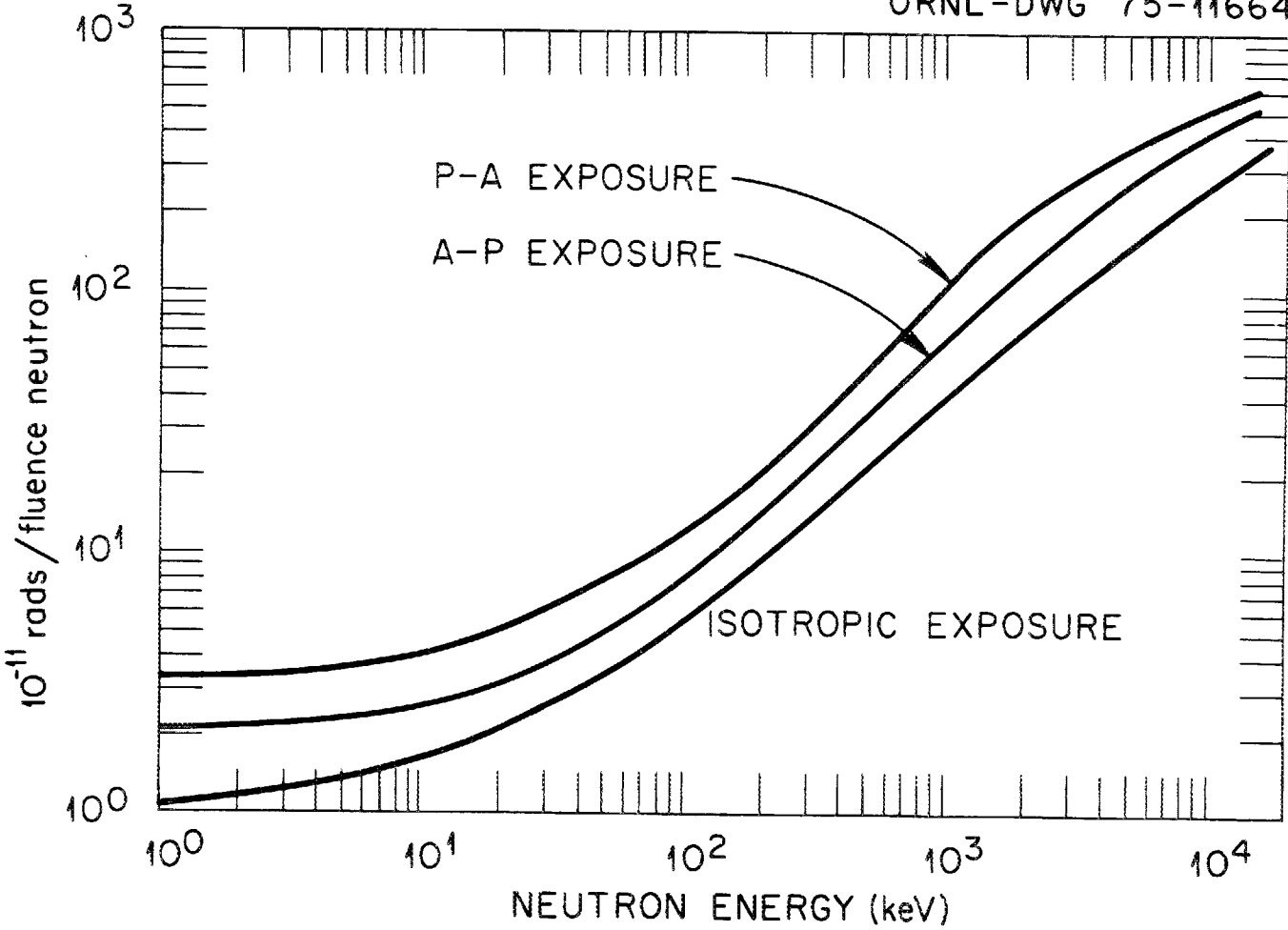


Fig. 8. Dose from Recoil Ions to the Active Marrow as Predicted by the CHORD Concept.

weight hydrogen and has a specific gravity of unity, while bone tissue contains about one-half the weight percentage of hydrogen as does muscle tissue but has about twice the specific gravity of muscle tissue so that the hydrogen atomic density is not very different for the two types of biological tissue. Lung tissue has a specific gravity of only about 0.3 and the hydrogen atomic density, therefore, is quite different; however, most critical organs of interest are either distant from the lung tissue or closer to an irradiated surface so that the penetration distance in grams/cm² is less than the other portion of the ray of travel that passes through a section of the lungs. Based on depth-dose curves from some of our previous calculations (Jones et al., 1973), it is believed that most regions of variable specific gravity do not significantly influence the application of the method of CHORDs, unless one is specifically interested in dose to a volume of lung tissue.

Other CHORD Applications

Figure 9 illustrates a proposed dosimeter or "riskmeter" in which the relative settings of the outer two dials select the appropriate CHORD distribution and the inner two dials select the insult (depth-dose) curve for the energy and type of incident radiation. Alun Jones (1966) suggested that dosimetry should be approached by matching variations in dose or risk with scattering, absorption, and attenuation; however, the CHORD method seems to permit this same precision of matching variability on a simplified macroscopic level.

Hopefully a schema such as incorporated into Figure 9 would render the absorbed dose index, D_I , and dose equivalent index, H_I , for

ORNL-DWG 75-277

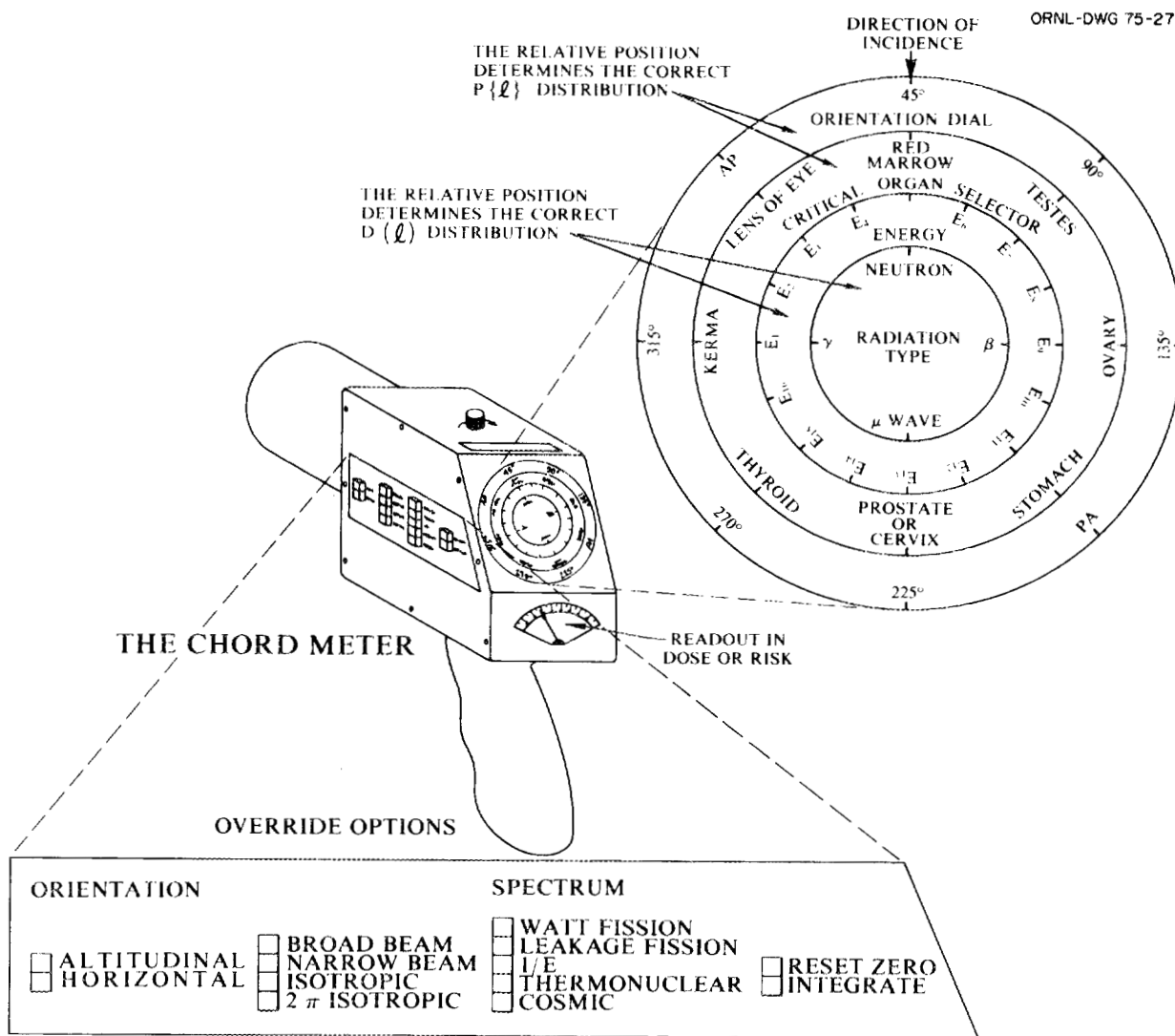


Fig. 9. Critical Human Organ Radiation Dosimeter.

the standard ICRU 30 cm sphere (ICRU, 1971) even less useful than it already is, because by using CHORD density functions plus standard insult (multicollision depth-dose) curves, a health physicist or medical technician could easily and quickly estimate exposure values to any biological tissue at risk. It is also becoming apparent that significant calculational and experimental efforts will soon be directed to the estimation of tissue risk due to microwave irradiations and the availability of $p\{\ell\} d\ell$ distributions should be helpful.

Conclusions

In summary, the method of CHORDs permits rapid "critical organ" dose estimation and helps to circumvent some of the problems of relating organ dose or risk to readings from meters or film badges. A personal dosimeter measures exposure at the surface of the chest; the measured exposure corresponds neither to the exposure in free space nor to the organ or whole body dose and area dosimeters determine only free space exposure (Piesch, 1967). Alun Jones (1966, 1964) pointed out that a survey meter or personal dosimeter may overestimate the insult to the active marrow by a factor of 10 or underestimate by a factor of 6. In spatially dependent radiation fields, or for exposure to broad beam sources having an orientation other than A-P, it is usually very difficult to have an accurate risk estimate because of normalization to an inaccurate or shielded reading taken at the location of the chest.

Acknowledgments

This paper is heavily dependent upon the experimental work of Wilson, Carruthers, Facey and Alun Jones for the discussion of the results and as a means of estimating the validity of the CHORD concept. It is also necessary to acknowledge the helpful suggestions and data supplied by Alun Jones and J. W. Poston.

References

- Clifford, C. E., and Facey, R. A., 1970, Health Physics 18, 217.
- Facey, R. A., 1968, Health Physics 14, 557.
- Fair, M., 1967, in Principles of Radiation Protection, Ed. K. Z. Morgan and J. E. Turner, Chap. 3 (John Wiley and Sons).
- ICRP Publication 6, 1964, Recommendations of the International Commission on Radiological Protection, (Pergamon Press).
- ICRP Publication 23, 1975, Report of the Task Group on Reference Man, (Pergamon Press).
- ICRU Report 19, 1971, Radiation Quantities and Units.
- Jones, A. R., 1964, AECL-2240.
- Jones, A. R., July 30, 1975, Personal communication to T. D. Jones.
- Jones, T. D., Auxier, J. A., Snyder, W. S., and Warner, G. G., 1973, Health Physics 24, 241.
- Piesch, E., 1968, Health Physics 15, 145.
- Poston, J. W., 1972, Personal communication of fluence per unit exposure conversion factors for Reference Man tissue composition.
- Radiological Health Handbook, 1970, U.S. Department of Health, Education, and Welfare, Public Health Service Consumer Protection and Environmental Health Service, Rockville, MD.
- Spiers, F. W., 1966, Rad. Research 28, 624.
- Wald, N., 1975, "Newer Biological Indicators of Radiation Damage," Refresher course given at Annual Meeting of Health Physics Society, July 13-17, 1975.
- Wilson, R., and Carruthers, J. A., Health Physics 7, 171, 1962.

INTERNAL DISTRIBUTION

- 1- 2. Central Research Library
- 3. Document Reference Section, CRL
- 4- 6. Laboratory Records
- 7. Laboratory Records, ORNL, RC
- 8. ORNL Patent Office
- 9. J. A. Auxier
- 10. J. L. Hwang
- 11. D. G. Jacobs
- 12-17. T. D. Jones
- 18-22. G. D. Kerr
- 23. J. W. Poston
- 24. C. R. Richmond
- 25. D. K. Trubey

EXTERNAL DISTRIBUTION

- 26-52. Technical Information Center, Townsite
- 53. Research and Technical Support Division, ORO, ERDA
- 54. L. R. Allen, Radiation Effects Research Foundation, 5-2 Hijiyama Koen, Hiroshima 730, Japan
- 55. Lowell Anderson, Dept. of Medical Physics, Memorial Hospital for Cancer and Allied Diseases, Sloan-Kettering Institute for Cancer Research, New York, NY
- 56. T. W. Armstrong, Science Applications, Inc., P. O. Box 2351, 1200 Prospect Street, La Jolla, CA 92037
- 57. F. H. Attix, Code 6603 A, Nucl. Science Div., Naval Research Lab., Washington, DC 20390
- 58. Donald E. Barber, Environmental Health, School of Public Health, 1325 Mayo Memorial Bldg., Minneapolis, MN 55455
- 59. G. W. Beebe, National Academy of Sciences, Washington, DC 20418
- 60. David E. Bernhardt, EPA, Box 15027, Las Vegas, NV 89114
- 61. Tom B. Borak, Biology and Medical Division, Argonne National Lab., 9700 South Cass Avenue, Argonne, IL 60439
- 62. James T. Brennan, University Hospital, Dept. of Radiology, 3400 Spruce Street, Philadelphia, PA 19104
- 63. H. D. Bruner, USERDA, Washington, DC 20545
- 64. W. W. Burr, Jr., USERDA, Washington, DC 20545
- 65. R. L. Butenhoff, USERDA, Washington, DC 20545
- 66. A. B. Chilton, University of Illinois, Urbana, IL
- 67. C. E. Clifford, Defense Research Establishment, Defense Research Board, Ottawa 4, Canada
- 68. George Cowper, Head, Health Physics Branch, Atomic Energy of Canada, Ltd., Chalk River Nuclear Lab., Chalk River, Ontario KOJ IJO, Canada
- 69. Roger Cloutier, Special Training Division, ORAU
- 70. W. G. Cross, Atomic Energy of Canada, Ltd., Chalk River Nuclear Lab., Chalk River, Ontario KOJ IJO, Canada

71. Desmond R. Davy, AAEC, HPR Section, Private Mail Bag, Sutherland N.S.W., Australia
72. J. A. Dennis, National Rad. Prot. Board, Harwell, Berkshire, England
73. Marc H. Dousset, Center d'Etudes Nucleaire, Department de la Protection Sanitaire, Service d'Hygiene Atomique, B.P.N^o 6, Fontenay - aux - Roses, France
74. R. A. Facey, Defense Research Establishment, Defense Research Board, Ottawa 4, Canada
75. S. B. Field, MRC Cyclotron Unit, Hammersmith Hospital, London, England
76. S. C. Finch, Radiation Effects Research Foundation, 5-2 Hijiyama Koen, Hiroshima 730, Japan
77. N. A. Frigerio, Argonne National Lab., 9700 South Cass Avenue, Argonne, IL 60439
78. R. V. Griffith, Lawrence Livermore Lab., University of California, P. O. Box 808, Livermore, CA 94550
79. Ferenc Hajnal, HASL, ERDA, 376 Hudson Street, New York, NY 10014
80. Dale Hankins, 312 Portrillo Drive, Los Alamos, NM 87544
81. Tadashi Hashizume, National Institute of Radiological Sciences, Chiba 280, Japan
82. William R. Hendee, Dept. of Radiology, University of Colorado Medical Center, 420 East Ninth Avenue, Denver, Colorado 80220
83. G. H. Herling, Code 6665, Navy Department, Naval Research Lab., Washington, DC 20390
84. H. E. Ing, Atomic Energy of Canada, Ltd., Chalk River Nuclear Lab., Chalk River, Ontario K0J 1J0, Canada
85. H. Jammet, Commissariat a l'Energie Atomique, Centre d'Etudes Nucleaire de Fontenay - aux - Roses, France
86. A. R. Jones, Health Physics Branch, Atomic Energy of Canada, Ltd., Chalk River Nuclear Lab., Chalk River, Ontario K0J 1J0, Canada
87. Dean Kaul, Science Applications, 5005 Newport Drive, Suite 305, Rolling Meadows, IL 60008
88. Sadahisa Kawamoto, Radiation Effects Research Foundation, 164 Sakurababa-machi, Nagasaki 850, Japan
89. T. J. Kennedy, Jr., National Academy of Sciences, Washington, DC 20418
90. Laszlo Koblinger, Health Physics Dept., Central Research Institute for Physics, P. O. Box 49, 1525 Budapest, Hungary
91. Andrzej Kreft, Institute of Nuclear Technology, Academy of Mining and Metallurgy, Cracow, Al. Mickiewicza 30, Poland
92. Lawrence H. Lanzl, The Franklin McLean Memorial Research Institute, University of Chicago, 950 E. 59th Street, Chicago, IL 60637
93. R. C. Lawson, UKAEA, Chapelcross, Annon, Scotland
94. J. L. Liverman, USERDA, Washington, DC 20545
95. Z. Makra, Central Research Institute for Physics, Budapest XII, Konkoly Thege ut, Hungary
96. Sidney Marks, USERDA, Washington, DC 20545
97. C. W. Mays, Radiobiology Lab., University of Utah, Salt Lake City, Utah 84112

98. P. H. McGinley, Emory University Clinic, Department of Rad. Therapy, 1365 Clifton Rd., N.E., Atlanta, GA 30322
- 99-108. I. M. Moriyama, Radiation Effects Research Foundation, 5-2 Hijiyama Koen, Hiroshima 730, Japan
109. Ladislov Musilek, Technical University of Prague, Faculty of Technical and Nuclear Physics, Brehovd 7 - Praha 1, Czechoslovakia
110. Dieter Nachtigall, Stahlschutz, Euratom 2 BKM, Steenweg naar, Retie, Geel/Belgium
111. Keren O'Brien, Health and Safety Lab., USERDA, New York, NY 10014
112. Ing. F. Pernicka, Laboratory for Radiological Dosimetry of the Czechoslovak Academy of Sciences, Praha 8, Na Truhlance 39/2a Czechoslovakia
113. E. Piesch, Karlsruhe Nuclear Research Center, Rad. Monitoring Service, Federal Republic of Germany
114. S. Pretre, Research Institute for Protective Construction, 8001 Zurich, Switzerland
115. H. H. Rossi, Professor of Radiology, College of Physicians and Surgeons of Columbia University, 630 West 168th Street, New York, NY 10032
116. W. J. Russell, Radiation Effects Research Foundation, 5-2 Hijiyama Koen, Hiroshima 730, Japan
117. E. L. Saenger, Radioisotope Lab., Cincinnati General Hospital and University of Cincinnati College of Medicine, Cincinnati, OH 45267
118. J. W. Smith, AERE, Harwell, Didcot, Berks., England
119. Kenji Takeshita, Research Institute for Nuclear Medicine and Biology, Hiroshima University, Hiroshima 734, Japan
120. Arnie Warshawsky, U.S. Army Agency, Fort Bliss, El Paso, TX
121. D. E. Watt, UKAEA, Chapelcross, Annon, Scotland
122. F. S. Williamson, Division of Biological and Medical Research, Argonne National Lab., 9700 South Cass Avenue, Argonne, IL 60439
123. R. Wilson, Defense Research Chemical Laboratory, Ottawa, Canada
124. R. W. Wood, USERDA, Washington, DC 20545
125. Hisao Yamashita, Radiation Effects Research Foundation, 5-2 Hijiyama Koen, Hiroshima 730, Japan
126. T. O. Young, Atomic Weapons Research Establishment, Bldg. A-29.1, Aldermaston, Reading RG74PR, United Kingdom